Signal Processing 116 (2015) 152–158

Contents lists available at ScienceDirect

Signal Processing

journal homepage: www.elsevier.com/locate/sigpro

Fast communication

Tensor-based real-valued subspace approach for angle estimation in bistatic MIMO radar with unknown mutual coupling

Xianpeng Wang, Wei Wang*, Jing Liu, Qi Liu, Ben Wang

College of Automation, Harbin Engineering University, Harbin 150001, China

ARTICLE INFO

Article history:
Received 17 June 2014
Received in revised form
17 March 2015
Accepted 25 March 2015
Available online 1 April 2015

Keywords:
Multiple-input multiple-output radar
Angle estimation
Real-valued signal subspace
Higher-order singular value decomposition
Mutual coupling

ABSTRACT

In this paper, a tensor-based real-valued subspace approach for joint direction of departure (DOD) and direction of arrival (DOA) estimation in bistatic MIMO radar with unknown mutual coupling is proposed. Exploiting the inherent multidimensional structure of received data after matched filtering, a third-order measurement tensor signal model is formulated. For eliminating the effect of the unknown mutual coupling, a sub-tensor can be extracted from the third-order measurement tensor by taking advantage of the banded symmetric Toeplitz structure of the mutual coupling matrix (MCM). Then the sub-tensor can be turned into a real-valued one by forward–backward averaging and unitary transformation, and a real-valued signal subspace is constructed to estimate the DOD and DOA by the higher-order singular value decomposition (HOSVD). Owing to utilize the multidimensional structure of received data and forward–backward averaging technique, the proposed method has better angle estimation performance than MUSIC-Like and ESPRIT-Like algorithms. Furthermore, the proposed method is suitable for coherent targets. Simulation results verify the effectiveness and advantage of the proposed method.

1. Introduction

Angle estimation problem is the most fundamental aspect in array processing applications [1], and many angle estimation techniques have been developed for the classical array processing, such as single-input multiple-output (SIMO) configuration [2,3]. Recently, a novel array processing configuration, named as multiple input multiple output (MIMO) radar, has opened new opportunities in parameter estimation, especially for joint direction of departure (DOD) and direction of arrival (DOA) estimation. MIMO radar can be divided into two classes: statistical MIMO radar [4] and collocated MIMO radar [5]. In the statistical MIMO radar, both of the transmit and receive antennas are widely spaced to achieve the spatial diversity gain. The collocated MIMO radar is composed of colocated transmit and receive antennas, which can form a virtual array with large aperture in the receiver, provide high-resolution spatial spectral estimation. In this paper, we focus on colocated MIMO radar.

In recent years, direction of departure (DOD) and direction of arrival (DOA) estimation problem in bistatic MIMO radar with colocated antennas has attracted more and more attention, and a lot of algorithms have been presented for this issue [6–10]. In [6], a two-dimensional spatial searching technique based on Capon estimator is proposed to estimate DOD and DOA, where the DOD and DOA are paired automatically. However, high computational burden is due to the two-dimensional spatial searching. In order to avoid the

* Corresponding author.
E-mail address: wangwei407@hrbeu.edu.cn (W. Wang).

http://dx.doi.org/10.1016/j.sigpro.2015.03.020
0165-1684/

procedure of spatial searching, the estimation of signal parameters via rotational invariance technique (ESPRIT) is applied for both the transmit array and receive array in bistatic MIMO radar [7], then the DOD and DOA can be achieved by two independent ESPRITs. Thus, the additional pairing procedure is required. Another ESPRIT algorithm with automatic pairing is presented in [8], which provides comparable angle estimation performance with lower computational complexity compared with the method in [7]. Moreover, exploiting the characteristic of non-circular signals, the conjugate ESPRIT (C-ESPRIT) and unitary conjugate ESPRIT are proposed in [9,10], which provide better angle estimation performance than ESPRIT-based methods. On the other hand, considering the effect of mutual coupling in both the transmit array and receive array, the accuracy of angle estimation in [6–10] will be degraded remarkably. In order to solve this issue, the MUSIC-Like algorithm and ESPRIT-Like algorithm are presented to estimate the angle and mutual coupling for bistatic MIMO radar in [11,12], respectively. However, all the methods mentioned above are required to stack the received data into a special structure matrix, which ignore the multidimensional structure inherence in the received data. Then the signal subspace or noise subspace can be estimated by eigenvalue decomposition (EVD) of the covariance matrix or singular value decomposition (SVD) of the received data. In [13,14], the multidimensional structure of the received data in bistatic MIMO radar is considered for improving the angle estimation performance. Compared with conventional ESPRIT algorithm, the multi-SVD technique in [14] provides better angle estimation, especially in low SNR region and limited snapshots. Unfortunately, the method in [14] is not suitable for the angle estimation in the presence of mutual coupling.

In this paper, we proposed a tensor-based real-valued subspace approach for joint DOD and DOA estimation in bistatic MIMO radar with unknown mutual coupling. Firstly, a third-order measurement tensor signal model is formulated by utilizing the multidimensional structure inherence in received data after matched filters. Then exploiting the special structure of the mutual coupling matrix (MCM), a sub-tensor without the effect of the mutual coupling is extracted from the third-order measurement tensor, and this sub-tensor can be mapped into a real-valued one by forward–backward averaging and unitary transformation. Finally, the higher order SVD (HOSVD) tensor decomposition technique is used to estimate the real-valued signal subspace. The DOD and DOA can be obtained by combining with the real-valued subspace based methods, such as unitary MUSIC and unitary ESPRIT, where the DOD and DOA are paired automatically. Due to exploit of the multidimensional structural inherence in received data and the forward–backward averaging technique, the proposed method provides better angle estimation performance than both MUSIC-Like and ESPRIT-Like algorithms. Moreover, the proposed method is suitable for coherent targets.

Notation: $(\cdot)^{\mathrm{H}}$, $(\cdot)^{\mathrm{T}}$, $(\cdot)^{-1}$, and $(\cdot)^{*}$ denote conjugate-transpose, transpose, inverse, conjugate, respectively. $\otimes$ and $\odot$ denote the Kronecker product operation and Khatri–Rao product operation. Toeplitz $\{\mathbf{r}\}$ denotes the symmetric Toeplitz matrix constructed by the vector $\mathbf{r}$. diag $(\cdot)$ denotes the diagonalization operation and blkdiag$\{\mathbf{r}_1, \mathbf{r}_2\}$ denotes a block-diagonal matrix with $\mathbf{r}_1$ and $\mathbf{r}_2$ being its diagonal submatrices. $\mathbf{I}_K$ denotes the $K \times K$ identity matrix, and $\mathbf{0}_{L\times K}$ is the $L \times K$ zero matrix.

2. Tensor basics and signal model

Tensor basics: First, we introduce several tensor operations, which refer to [15,16].

Definition 1 (*Matrix unfolding*). Let $\mathcal{X} \in \mathbb{C}^{I_1 \times I_2 \cdots \times I_N}$ be a tensor, and the mode-n matrix unfolding of a tensor $\mathcal{X}$ is denoted by $[\mathcal{X}]_{(n)}$. The $(i_1, i_2, \ldots, 1_N)$th element of $\mathcal{X}$ maps to the (i_n, j) th element of $\mathcal{X}$, where $j = 1 + \sum_{k=1, k\neq n}^{N} (i_k - 1) J_k$ with $J_k = \prod_{m=1, m\neq n}^{k-1} I_m$.

Definition 2 (*Mode-n tensor-matrix product*). The mode-n product of $\mathcal{X} \in \mathbb{C}^{I_1 \times I_2 \times \cdots \times I_N}$ with a matrix $\mathbf{A} \in \mathbb{C}^{J_n \times I_n}$ is denoted by $\mathcal{Y} = \mathcal{X} \times_n \mathbf{A}$, where $\mathcal{Y} \in \mathbb{C}^{I_1 \times I_2 \times \cdots \times I_{n-1} \times J_n \times I_{n+1} \times \cdots \times I_N}$ and $[\mathcal{Y}]_{i_1, i_2, \ldots, i_{n-1} j_n i_{n+1}, \ldots, i_N} = \sum_{i_n=1}^{I_n} [\mathcal{X}]_{i_1, i_2, \ldots, i_{n-1}, i_n, i_{n+1}, \ldots, i_N} \cdot [\mathbf{A}]_{j_n, i_n}$

Definition 3 (*The properties of the mode product*). The properties of the mode product are shown as follow [16]:

$$\begin{aligned} &\mathcal{X} \times_n \mathbf{A} \times_m \mathbf{B} = \mathcal{X} \times_m \mathbf{B} \times_n \mathbf{A}, \quad m \neq n \\ &\mathcal{X} \times_n \mathbf{A} \times_n \mathbf{B} = \mathcal{X} \times_n (\mathbf{B}\mathbf{A}) \end{aligned} \tag{1}$$

$$\begin{aligned} &[\mathcal{X} \times_1 \mathbf{A}_1 \times_2 \mathbf{A}_2 \times \cdots \times_N \mathbf{A}_N]_{(n)} \\ &= \mathbf{A}_n \cdot [\mathcal{X}]_{(n)} \cdot \left[\mathbf{A}_N \otimes \ldots \otimes \mathbf{A}_{n+1} \otimes \mathbf{A}_{n-1} \otimes \ldots \otimes \mathbf{A}_2 \otimes \mathbf{A}_1\right]^{\mathrm{T}} \end{aligned} \tag{2}$$

Tensor-based signal model: Consider a narrowband bistatic multiple-input multiple-output (MIMO) radar system equipped with M transmit antennas and N receive antennas. Both of the transmit array and receive array are composed of half-wavelength spaced uniform linear arrays (ULA). At the transmit array, M antennas are used to transmit M orthogonal narrowband waveforms $\mathbf{S} = [\mathbf{s}_1, \mathbf{s}_2, \ldots, \mathbf{s}_M]^{\mathrm{T}} \in \mathbb{C}^{M\times J}$, where J is the number of samples per pulse period. All the targets are modeled as a point-scatterer in the far-field, and we assume that there exists P uncorrelated targets in the same range-bin of interest. The direction of departure (DOD) and direction of arrival (DOA) of the pth target can be denoted as φ_p and θ_p, respectively. Consider the effect of mutual coupling in both transmit array and receive array, and it is also assumed that the number of nonzeros mutual coupling coefficients of both the transmit and receive arrays is $K+1$ with $\min\{M, N\} > 2K$. Then the mutual coupling matrices of the transmit and receive arrays can be modeled as banded symmetric Toeplitz matrices, which can be expressed as [11,12]

$$\begin{aligned} &\mathbf{C}_t = \text{toeplitz}\{[c_{t0}, c_{t1}, \ldots, c_{tK}, 0, \ldots, 0]\} \in \mathbb{C}^{M\times M} \\ &\mathbf{C}_r = \text{toeplitz}\{[c_{r0}, c_{r1}, \ldots, c_{rK}, 0, \ldots, 0]\} \in \mathbb{C}^{N\times N} \end{aligned} \tag{3}$$

where $c_{ik}, (i = r, t, k = 0, 1, \ldots, K)$ is the mutual coupling coefficient, which is a factor concerned with the distance between two elements [11] and satisfied with $0 < |c_{tK}| < \cdots < |c_{t1}| < |c_{t0}| = 1$. Then the output of the receive array can be written as [11,12]

$$\mathbf{X}(t_l) = [\mathbf{C}_r \mathbf{A}_r] \mathbf{\Sigma}_l [\mathbf{C}_t \mathbf{A}_t]^{\mathrm{T}} \mathbf{S} + \mathbf{W}(t_l), \quad l = 1, 2, \ldots, L \tag{4}$$

where $\mathbf{X}(t_l) \in \mathbb{C}^{N\times K}$ is the received data for the lth pulse period, L is the number of pulses. $\mathbf{A}_r = [a_r(\theta_1), \ldots, a_r(\theta_P)]$ and

$\mathbf{A}_t=[a_t(\varphi_1),\ldots,a_t(\varphi_P)]$ are the receive steering matrix and the transmit steering matrix, respectively. $\mathbf{a}_r(\theta_p)=[1,e^{j\pi\sin\theta_p},\ldots,e^{j\pi(N-1)\sin\theta_p}]^{\mathrm{T}}$ and $\mathbf{a}_t(\varphi_p)=\left[1,e^{j\pi\sin\varphi_p},\ldots,e^{j\pi(M-1)\sin\varphi_p}\right]^{\mathrm{T}}(p=1,2,\ldots,P)$ are the receive steering vector and the transmit steering matrix, respectively. $\mathbf{\Sigma}_l=\mathrm{diag}(\mathbf{c}_l)$ is composed of $\mathbf{c}_l=\left[\beta_1e^{j2\pi f_{d1}l},\beta_2e^{j2\pi f_{d2}l},\ldots,\beta_Pe^{j2\pi f_{dp}l}\right]^{\mathrm{T}}$, $\left\{\beta_p\right\}_{p=1}^{P}$ and $\left\{f_{dp}\right\}_{p=1}^{P}$ are the RCS fading coefficients and the targets Doppler frequency, respectively. In this paper, we consider that the RCS fading coefficients $\left\{\beta_p\right\}_{p=1}^{P}$ are constant in all pulses, which means that the RCS of all targets is the Swerling I model. $\mathbf{W}$ is assumed to be temporally and spatially white, and uncorrelated from the targets. Exploiting the orthogonality of the transmitted waveforms shown as $(1/J)\mathbf{S}\mathbf{S}^{\mathrm{H}}=\mathbf{I}_M$, Eq. (2) is right multiplied by $(1/J)\mathbf{S}^{\mathrm{H}}$, then the output of matched filters is

$$\mathbf{Y}(t_l)=[\mathbf{C}_r\mathbf{A}_r]\mathbf{\Sigma}[\mathbf{C}_t\mathbf{A}_t]^{\mathrm{T}}+\mathbf{N}(t_l),\quad l=1,2,\ldots,L \tag{5}$$

where $\mathbf{Y}(t_l)=(1/J)\mathbf{X}(t_l)\mathbf{S}^{\mathrm{H}}\in\mathbb{C}^{N\times M}$ and $\mathbf{N}=(1/J)\mathbf{W}\mathbf{S}^{\mathrm{H}}$. Based on the matrix unfolding of tensor in Definition 1, the received data matrix in Eq. (5) for each pulse can be considered as a slice along the direction of pulse (the third-dimension). Then we stack the matrices $\mathbf{Y}(t_l)(l=1,2,\ldots,L)$ along the third-dimension to built the $N\times M\times L$ measurement tensor $\mathcal{Y}$. Exploiting the matrix unfolding technique to tensor $\mathcal{Y}$, we have

$$[\mathcal{Y}]_{(3)}^{\mathrm{T}}=[\mathbf{C}_t\mathbf{A}_t]\odot[\mathbf{C}_r\mathbf{A}_r]\overline{\mathbf{S}}+\overline{\mathbf{N}} \tag{6}$$

where $\overline{\mathbf{S}}=[\mathbf{c}_1,\mathbf{c}_2,\ldots,\mathbf{c}_l]\in\mathbb{C}^{P\times L}$ and $\overline{\mathbf{N}}=[\mathrm{vec}(\mathbf{N}(t_1)),\ldots,\mathrm{vec}(\mathbf{N}(t_L))]\in\mathbb{C}^{MN\times L}$.

Remark 1. As shown in [11,12], the subspace methods are based on Eq. (6), which indicates that these methods only use "one-dimensional" information and ignore the multi-dimensional structure of the measurement tensor $\mathcal{Y}$. Thus, the angle estimation performance is limited with lower SNR and pulses. Additionally, the method in [13] is not suitable anymore owing to the mutual coupling.

3. Tensor-based real-valued subspace approach for angle estimation with unknown mutual coupling

Exploiting the structure characteristic of both the mutual coupling matrices $\mathbf{C}_r$ and $\mathbf{C}_t$ in Eq. (3), two selection matrices are defined as [12]

$$\mathbf{J}_1=[\mathbf{0}_{(M-2K)\times K}\quad\mathbf{I}_{M-2K}\quad\mathbf{0}_{(M-2K)\times K}] \tag{7a}$$

$$\mathbf{J}_2=[\mathbf{0}_{(N-2K)\times K}\quad\mathbf{I}_{N-2K}\quad\mathbf{0}_{(N-2K)\times K}] \tag{7b}$$

Then, multiplying the selection matrices $\mathbf{J}_2$ and $\mathbf{J}_1$ on the left and right sides of $\mathbf{Y}(t_l)(l=1,2,\ldots,L)$, respectively, we have

$$\overline{\mathbf{Y}}(t_l)=\mathbf{J}_2\mathbf{Y}(t_l)\mathbf{J}_1,\quad l=1,2,\ldots,L \tag{8}$$

and the $(\overline{n},\overline{m})$ element of $\overline{\mathbf{Y}}(t_l)$ can be expressed as

$$[\overline{\mathbf{Y}}(t_l)]_{\overline{n},\overline{m}}=\sum_{p=1}^{P}s_{p,l}\nu_{rp}\nu_{tp}e^{j\pi(\overline{n}-1)\sin\theta_p}e^{j\pi(\overline{m}-1)\sin\varphi_p}+[\overline{\mathbf{N}}(t_l)]_{\overline{n},\overline{m}} \tag{9}$$

where $1\le\overline{n}\le\overline{N}=N-2K$, $1\le\overline{m}\le\overline{\overline{M}}=M-2K$ and $\min\{\overline{N}(\overline{M}-1),\overline{M}(\overline{N}-1)\}\ge P$. $s_{p,l}=\beta_pe^{j2\pi f_{dp}l}$, $\nu_{rp}=\sum_{k=-K}^{K}c_{r|k|}e^{j\pi(k+K)\sin\theta_p}$, $\nu_{tp}=\sum_{k=-K}^{K}c_{t|k|}e^{j\pi(k+K)\sin\varphi_p}$ and $\overline{\mathbf{N}}(t_l)=\mathbf{J}_2\mathbf{N}(t_l)\mathbf{J}_1$. According to Eq. (7a) and (7b), it can be concluded that $\nu=\sum_{p=1}^{P}\nu_{rp}\nu_{tp}$ is constant for each element of $\overline{\mathbf{Y}}(t_l)$, which indicates that the effect of mutual coupling is eliminated by the linear transformation in Eq. (8). Then Eq. (8) can be rewritten as

$$\overline{\mathbf{Y}}(t_l)=\overline{\mathbf{A}}_r\overline{\mathbf{\Sigma}}\overline{\mathbf{A}}_t^{\mathrm{T}}+\overline{\mathbf{N}}(t_l)\quad l=1,2,\ldots,L \tag{10}$$

where $\overline{\mathbf{A}}_r$ and $\overline{\mathbf{A}}_t$ are the first $\overline{N}$ and $\overline{M}$ rows of $\mathbf{A}_r$ and $\mathbf{A}_t$, respectively. $\overline{\mathbf{\Sigma}}=\mathrm{diag}([\nu\beta_1e^{j2\pi f_{d1}l},\nu\beta_2e^{j2\pi f_{d2}l},\ldots,\nu\beta_Pe^{j2\pi f_{dp}l}])$. The operation in Eq. (8) is only considered for one slice of the measurement tensor $\mathcal{Y}$. Now, we extend the linear transformation to the measurement tensor $\mathcal{Y}$. According to Definition 2, a novel measurement sub-tensor $\overline{\mathcal{Y}}$ can be extracted from the measurement tensor $\mathcal{Y}$, which is shown as

$$\overline{\mathcal{Y}}=\mathcal{Y}\times_1\mathbf{J}_2\times_2\mathbf{J}_1 \tag{11}$$

After exploiting the operation in Eq. (11), each slice of $\overline{\mathcal{Y}}$ along the direction of pulse corresponds to the data $\overline{\mathbf{Y}}(t_l)(l=1,2,\ldots,L)$ in (10). Thus, the measurement sub-tensor data $\overline{\mathcal{Y}}$ is robust in the presence of mutual coupling. Then, exploiting the forward–backward averaging technique to the sub-tensor, we have

$$\mathcal{Z}=[\overline{\mathcal{Y}}\sqcup_3(\overline{\mathcal{Y}}^{*}\times_1\mathbf{\Pi}_{\overline{N}}\times_2\mathbf{\Pi}_{\overline{M}}\times_3\mathbf{\Pi}_L)] \tag{12}$$

where $[\mathcal{A}\sqcup_n\mathcal{B}]$ denotes the concatenation of $\mathcal{A}$ and $\mathcal{B}$ along the nth mode and $\mathbf{\Pi}_n$ is the $n\times n$ exchange matrix having ones on its antidiagonal and zeros elsewhere. After using the forward–backward averaging technique, the tensor $\mathcal{Z}$ is centro-Hermitian [17], and it can be turned into the set of real-valued tensors by using unitary transformation. The real-valued tensor can be obtained as

$$\mathcal{Z}_{rv}=\mathcal{Z}\times_1\mathbf{U}_{\overline{N}}^{\mathrm{H}}\times_2\mathbf{U}_{\overline{M}}^{\mathrm{H}}\times_3\mathbf{U}_{2L}^{\mathrm{H}} \tag{13}$$

where $\mathbf{U}_{2K+1}$ is unitary matrix and defined as

$$\mathbf{U}_{2K+1}=\frac{1}{\sqrt{2}}\begin{bmatrix}\mathbf{I}_K & 0 & j\mathbf{I}_K\\ \mathbf{0}_{1\times K} & \sqrt{2} & \mathbf{0}_{1\times K}\\ \mathbf{\Pi}_K & 0 & -j\mathbf{\Pi}_K\end{bmatrix} \tag{14}$$

and $\mathbf{U}_{2K}$ is easily obtained from $\mathbf{U}_{2K+1}$ by omitting its center row and center column. Then the HOSVD of $\mathcal{Z}_{rv}$ is given by [14]

$$\mathcal{Z}_{rv}=\mathcal{G}_{rv}\times_1\mathbf{E}_1\times_2\mathbf{E}_2\times_3\mathbf{E}_3 \tag{15}$$

where $\mathcal{G}_{rv}\in\mathbb{R}^{\overline{N}\times\overline{M}\times 2L}$ is the core tensor. $\mathbf{E}_1\in\mathbb{R}^{\overline{N}\times\overline{N}}$, $\mathbf{E}_2\in\mathbb{R}^{\overline{M}\times\overline{M}}$ and $\mathbf{E}_3\in\mathbb{R}^{2L\times 2L}$ are real-valued unitary matrices, which are composed of the left singular vectors of the i-mode matrix unfolding of $\mathcal{Z}_{rv}$ as $[\mathcal{Z}_{rv}]_{(i)}=\mathbf{E}_i\mathbf{\Lambda}_i\mathbf{V}_i^{\mathrm{H}}(i=1,2,3)$, respectively. Since tensor $\mathcal{Z}_{rv}$ is rank-P, the real-valued subspace tensor of $\mathcal{Z}_{rv}$ can be defined by using truncated HOSVD of $\mathcal{Z}_{rv}$, which is expressed as

$$\mathcal{Z}_s=\mathcal{G}_s\times_1\mathbf{E}_{s1}\times_2\mathbf{E}_{s2} \tag{16}$$

where $\mathcal{G}_s=\mathcal{Z}_{rv}\times_1\mathbf{E}_{s1}^{\mathrm{H}}\times_2\mathbf{E}_{s2}^{\mathrm{H}}\times_3\mathbf{E}_{s3}^{\mathbf{H}}$ is the reduced core tensor, $\mathbf{E}_{si}(i=1,2,3)$ contains the first P dominant singular vectors of $\mathbf{E}_i$. Insertion of $\mathcal{G}_s$ into Eq. (16), and according to Eq. (1), we

have

$$\mathcal{Z}_s = \mathcal{Z}_{rv} \times_1 \mathbf{E}_{s1}\mathbf{E}_{s1}^{\mathrm{H}} \times_2 \mathbf{E}_{s2}\mathbf{E}_{s2}^{\mathrm{H}} \times_3 \mathbf{E}_{s3}^{\mathrm{H}} \tag{17}$$

Then based on Eq. (2), the real-valued signal subspace can be given as

$$\mathbf{E}_s = [\mathcal{Z}_s]_{(3)}^{\mathrm{T}} = (\mathbf{E}_{s2}\mathbf{E}_{s2}^{\mathrm{H}} \otimes \mathbf{E}_{s1}\mathbf{E}_{s1}^{\mathrm{H}})\mathbf{Z}\mathbf{E}_{s3}^{*} \tag{18}$$

where $\mathbf{Z} = [\mathcal{Z}_{rv}]_{(3)}^{\mathrm{T}}$.

Lemma 1. *The real-valued signal subspace $\mathbf{E}_s$ and real-valued steering matrix $\mathbf{U}_M^{\mathrm{H}}\overline{\mathbf{A}}_t \odot \mathbf{U}_N^{\mathrm{H}}\overline{\mathbf{A}}_r$ are spanned the same subspace, i.e., $\mathbf{E}_s = (\mathbf{U}_M^{\mathrm{H}}\overline{\mathbf{A}}_t \odot \mathbf{U}_N^{\mathrm{H}}\overline{\mathbf{A}}_r)\mathbf{T}$, where $\mathbf{T}$ is a full-rank matrix.*

Proof. Due to $[\mathcal{Z}_{rv}]_{(3)} = \mathbf{E}_3\Lambda_3\mathbf{V}_3^{\mathrm{H}}$, the SVD of $\mathbf{Z}$ can be expressed as $\mathbf{Z} = [\mathcal{Z}_{rv}]_{(3)}^{\mathrm{T}} \approx \mathbf{V}_{3s}^{*}\mathbf{\Lambda}_{3s}\mathbf{E}_{3s}^{\mathrm{T}}$. Then inserting $\mathbf{Z} \approx \mathbf{V}_{3s}^{*}\mathbf{\Lambda}_{3s}\mathbf{E}_{3s}^{\mathrm{T}}$ into Eq. (18), we have

$$\mathbf{E}_s = (\mathbf{E}_{s2}\mathbf{E}_{s2}^{\mathrm{H}} \otimes \mathbf{E}_{s1}\mathbf{E}_{s1}^{\mathrm{H}})\mathbf{V}_{3s}^{*}\mathbf{\Lambda}_{3s} \tag{19}$$

According to Eqs. (13)–(16), it can be concluded the fact that the real-valued $\mathbf{E}_{s1}$ and $\mathbf{E}_{s2}$ span the same signal subspace as the real-valued transmit steering matrix $\hat{\mathbf{A}}_t = \mathbf{U}_M^{\mathrm{H}}\overline{\mathbf{A}}_t$ and real-valued receive steering matrix $\hat{\mathbf{A}}_r = \mathbf{U}_N^{\mathrm{H}}\overline{\mathbf{A}}_r$. Additionally, the real-valued signal subspace $\mathbf{V}_{3s}^{*}$ can be expressed as $\mathbf{V}_{3s}^{*} = (\hat{\mathbf{A}}_t \odot \hat{\mathbf{A}}_r)\mathbf{T}_1$, where $\mathbf{T}_1$ is full-rank matrices. Additionally, the well-known characteristic of between the signal subspace and steering matrix can be shown as $\mathbf{E}_{s1}\mathbf{E}_{s1}^{\mathrm{H}} = \hat{\mathbf{A}}_r\left(\hat{\mathbf{A}}_r^{\mathrm{H}}\hat{\mathbf{A}}_r\right)^{-1}\hat{\mathbf{A}}_r^{\mathrm{H}}$ and $\mathbf{E}_{s2}\mathbf{E}_{s2}^{\mathrm{H}} = \hat{\mathbf{A}}_t\left(\hat{\mathbf{A}}_t^{\mathrm{H}}\hat{\mathbf{A}}_t\right)^{-1}\hat{\mathbf{A}}_t^{\mathrm{H}}$. Thus, inserting $\mathbf{V}_{3s}^{*} = (\hat{\mathbf{A}}_t \odot \hat{\mathbf{A}}_r)\mathbf{T}_1$ into Eq. (19), we have

$$\begin{aligned}\mathbf{E}_s &= (\mathbf{E}_{s2}\mathbf{E}_{s2}^{\mathrm{H}} \otimes \mathbf{E}_{s1}\mathbf{E}_{s1}^{\mathrm{H}})(\hat{\mathbf{A}}_t \odot \hat{\mathbf{A}}_r)\mathbf{T}_1\mathbf{\Lambda}_{3s} \\ &= (\mathbf{E}_{s2}\mathbf{E}_{s2}^{\mathrm{H}}\hat{\mathbf{A}}_t) \odot (\mathbf{E}_{s1}\mathbf{E}_{s1}^{\mathrm{H}}\hat{\mathbf{A}}_r)\mathbf{T}_1\mathbf{\Lambda}_{3s} \\ &= [\hat{\mathbf{A}}_t\left(\hat{\mathbf{A}}_t^{\mathrm{H}}\hat{\mathbf{A}}_t\right)^{-1}\hat{\mathbf{A}}_t^{\mathrm{H}}\hat{\mathbf{A}}_t] \odot [\hat{\mathbf{A}}_r\left(\hat{\mathbf{A}}_r^{\mathrm{H}}\hat{\mathbf{A}}_r\right)^{-1}\hat{\mathbf{A}}_r^{\mathrm{H}}\hat{\mathbf{A}}_r]\mathbf{T}_1\mathbf{\Lambda}_{3s} \\ &= (\hat{\mathbf{A}}_t \odot \hat{\mathbf{A}}_r)\mathbf{T}_1\mathbf{\Lambda}_{3s}\end{aligned} \tag{20}$$

Since both $\mathbf{T}_1$ and $\mathbf{\Lambda}_{3s}$ are full-rank matrix, $\mathbf{T} = \mathbf{T}_1\mathbf{\Lambda}_{3s}$ is full-rank matrix. Up to now, Lemma 1 is completely proved. According to Lemma 1, it can be concluded that the real-valued signal subspace $\mathbf{E}_s$ can be used to estimate DOD and DOA by combining with real-valued subspace methods, such as unitary MUSIC [18] and unitary ESPRIT [19]. The detail will be shown in the following.

Two-dimensional unitary MUSIC algorithm: Exploiting the orthogonality characteristic between the real-valued noise subspace and the real-valued steering vector, a two-dimensional unitary MUSIC spatial peak searching function can be constructed for DOD and DOA estimation, which is shown as

$$\mathrm{P}(\varphi,\theta) = \frac{1}{\left[\mathbf{U}_M^{\mathrm{H}}\overline{\mathbf{a}}_t(\varphi) \otimes \mathbf{U}_N^{\mathrm{H}}\overline{\mathbf{a}}_r(\theta)\right]^{\mathbf{H}}\mathbf{F}_n[\mathbf{U}_M^{\mathrm{H}}\overline{\mathbf{a}}_t(\varphi) \otimes \mathbf{U}_N^{\mathrm{H}}\overline{\mathbf{a}}_r(\theta)]} \tag{21}$$

where $\overline{\mathbf{a}}_t(\varphi)$ and $\overline{\mathbf{a}}_r(\theta)$ are composed of the fist $\overline{N}$ and $\overline{M}$ elements of $\mathbf{a}_t(\varphi)$ and $\mathbf{a}_r(\theta)$, respectively. $\mathbf{F}_n = \mathbf{I}_{\overline{N}\times\overline{M}} - \mathbf{E}_{so}\mathbf{E}_{so}^{\mathrm{H}}$, where $\mathbf{E}_{so}$ is the orthogonal basis of $\mathbf{E}_s$. Then the DOD and DOA can be obtained by searching the spatial peak of Eq. (21) and can be paired automatically.

Unitary ESPRIT algorithm: In order to adopt the unitary ESPRIT algorithm for DOD and DOA estimation, the real-valued signal subspace $\mathbf{E}_s$ can be divided into four parts, and there exist the following rotational invariance equation:

$$\mathbf{\Gamma}_2\mathbf{E}_s = \mathbf{\Gamma}_1\mathbf{E}_s\mathbf{\Psi}_t, \quad \mathbf{\Gamma}_4\mathbf{E}_s = \mathbf{\Gamma}_3\mathbf{E}_s\mathbf{\Psi}_r \tag{22}$$

where $\mathbf{\Gamma}_1 = \mathrm{Re}\{(\mathbf{U}_{\overline{M}-1} \otimes \mathbf{U}_{\overline{N}})\mathbf{J}_2^{\varphi}(\mathbf{U}_{\overline{M}} \otimes \mathbf{U}_{\overline{N}})\}$ and $\mathbf{\Gamma}_2 = \mathrm{Im}\{(\mathbf{U}_{\overline{M}-1} \otimes \mathbf{U}_{\overline{N}})\mathbf{J}_2^{\varphi}(\mathbf{U}_{\overline{M}} \otimes \mathbf{U}_{\overline{N}})\}$ with $\mathbf{J}_2^{\varphi} = [\mathbf{0}_{\overline{N}(\overline{M}-1)\times N}, \mathbf{I}_{\overline{N}(\overline{M}-1)}]$, $\mathbf{\Gamma}_3 = \mathrm{Re}\{(\mathbf{U}_{\overline{M}} \otimes \mathbf{U}_{\overline{N}-1})\mathbf{J}_4^{\theta}(\mathbf{U}_{\overline{M}} \otimes \mathbf{U}_{\overline{N}})\}$ and $\mathbf{\Gamma}_4 = \mathrm{Im}\{(\mathbf{U}_{\overline{M}} \otimes \mathbf{U}_{\overline{N}-1})\mathbf{J}_4^{\theta}(\mathbf{U}_{\overline{M}} \otimes \mathbf{U}_{\overline{N}})\}$ with $\mathbf{J}_4^{\theta} = \mathbf{I}_{\overline{M}} \otimes [\mathbf{0}_{(\overline{N}-1)\times 1}, \mathbf{I}_{(\overline{N}-1)}]$. $\mathbf{\Psi}_t = \Upsilon\mathbf{\Phi}_t\Upsilon^{-1}$ and $\mathbf{\Psi}_r = \Upsilon\mathbf{\Phi}_r\Upsilon^{-1}$ are the rotational invariance matrix, which contain the information of DOD and DOA, respectively, where $\mathbf{\Phi}_t = \mathrm{diag}([\tan(\pi \sin(\varphi_1)/2), \tan(\pi \sin(\varphi_2)/2), \ldots, \tan(\pi \sin(\varphi_P)/2))]$ and $\mathbf{\Phi}_r = \mathrm{diag}([\tan(\pi \sin(\theta_1)/2), \tan(\pi \sin(\theta_2)/2), \ldots, \tan(\pi \sin(\theta_P)/2))]$. Then $\mathbf{\Psi}_t$ and $\mathbf{\Psi}_r$ can be estimated by using least squares (LS) or the total least squares (TLS) algorithm in Eq. (22). In order to avoid the procedure of pairing operation, the pairing strategy in [20] can be utilized, which can be expressed as

$$\mathbf{\Psi}_t + j\mathbf{\Psi}_r = \Upsilon(\mathbf{\Phi}_t + j\mathbf{\Phi}_r)\Upsilon^{-1} \tag{23}$$

The diagonal matrix $\mathbf{\Phi}_t$ and $\mathbf{\Phi}_t$ can be obtained from the real and imaginary parts of the eigenvalues of $\mathbf{\Psi}_t + j\mathbf{\Psi}_r$. Then the DOD and DOA are paired automatically, and the DOD and DOA can be derived as

$$\hat{\varphi}_p = \arcsin(2\arctan(\Upsilon_{tp})/\pi), \quad p = 1, 2, \ldots, P \tag{24a}$$

$$\hat{\theta}_p = \arcsin(2\arctan(\Upsilon_{rp})/\pi), \quad p = 1, 2, \ldots, P \tag{24b}$$

where Υ_{tp} and Υ_{rp} are the pth diagonal element of $\mathbf{\Phi}_t$ and $\mathbf{\Phi}_t$, respectively. □

4. Related remarks and CRB

Remark 2. As shown in (19), the matrix-based subspace-methods [11,12] use the signal subspace $\mathbf{V}_{3s}^{*}$ to estimate the DOD and DOA, but the proposed method use the signal subspace $\mathbf{E}_s$ instead of $\mathbf{V}_{3s}^{*}$. In the absence of noise or the target number P is larger than $\overline{M}$ and $\overline{N}$, the signal subspace $\mathbf{E}_s$ and $\mathbf{V}_{3s}^{*}$ are same owing to both of $\mathbf{E}_{s1}\mathbf{E}_{s1}^{\mathrm{H}}$ and $\mathbf{E}_{s2}\mathbf{E}_{s2}^{\mathrm{H}}$ are unit matrix. Otherwise, they are different and the estimation of $\mathbf{E}_s$ is more accuracy than $\mathbf{V}_{3s}^{*}$. The main reason is that exploiting the multi-dimensional structure inherence in the received signal, the proposed method uses the HOSVD technique to suppress the noise more effectively compared with the traditional SVD/EVD approach. Thus, the angle estimation performance can be improved in the proposed method.

Remark 3. The computational complexity of the proposed method is analyzed as following. As shown in [21], for a $M \times N$ complexity matrix, the computational complexity of the truncated SVD to rank K is $O(MNK)$. On other hand, since the computational complexity of one multiplication between two complex-valued matrix generally requires four times that of between two real-valued ones, the computational complexity of real-valued operation can reduce about 75%. In the proposed method, the signal subspace $\mathbf{E}_s$ can be estimated by three truncated SVDs of matrix unfolding of the real-valued sub-sensor $\mathcal{Z}_{rv}$. The computational complexity of the proposed method is $O(3/4\overline{M}\overline{N}P)$, while the matrix-based subspace methods

(such as ESPRI-Like [12]) need $O(\overline{MNP})$ computational complexity to estimate the complex-valued signal subspace. Thus, the proposed method has similar computational complexity with the matrix-based subspace methods.

Cramer–Rao bound (*CRB*): According to [12], the CRB of angle estimation can be defined as

$$CRB=\frac{\sigma^2}{2}\left[\mathbf{J}_{\eta\eta}-\mathbf{J}_{\gamma\eta}\mathbf{J}_{\gamma\gamma}^{-1}\mathbf{J}_{\gamma\eta}^{\mathrm{T}}\right]^{-1} \tag{25}$$

where

$$\mathbf{J}_{\eta\eta}=\sum_{l=1}^{L}\mathrm{Re}\{\mathbf{D}_l^{\mathrm{H}}\boldsymbol{\Gamma}_{\bar{A}}^{\perp}\mathbf{D}_l\},\quad \mathbf{J}_{\gamma\eta}=\sum_{l=1}^{L}\mathrm{Re}\{\mathbf{D}_l^{\mathrm{H}}\boldsymbol{\Gamma}_{\bar{A}}^{\perp}\mathbf{H}_l\},\quad \mathbf{J}_{\gamma\gamma}=\sum_{l=1}^{L}\mathrm{Re}\{\mathbf{H}_l^{\mathrm{H}}\boldsymbol{\Gamma}_{\bar{A}}^{\perp}\mathbf{H}_l\}, \tag{26}$$

in which $\boldsymbol{\Gamma}_{\bar{A}}^{\perp}=\mathbf{I}_{MN}-{}'\mathbf{A}[\,\mathbf{A}^{\mathrm{H}}{}'\mathbf{A}]{}'\mathbf{A}^{\mathrm{H}}$ with ${}'\mathbf{A}=[\mathbf{C}_t\mathbf{A}_t]\odot[\mathbf{C}_r\mathbf{A}_r]$. $\mathbf{D}_l$ and $\mathbf{H}_l$ ar expressed as $\mathbf{D}_l=\left[\frac{\partial\check{\mathbf{b}}_1}{\partial\varphi_1},\ldots,\frac{\partial\check{\mathbf{b}}_P}{\partial\varphi_P},\frac{\partial\check{\mathbf{b}}_1}{\partial\theta_1},\ldots,\frac{\partial\check{\mathbf{b}}_P}{\partial\theta_P}\right]$ and $\mathbf{H}_l=\left(\left[\frac{\partial\mathbf{C}}{\partial a_{t1}},\ldots,\frac{\partial\mathbf{C}}{\partial a_{tK}},\frac{\partial\mathbf{C}}{\partial a_{r1}},\ldots,\frac{\partial\mathbf{C}}{\partial a_{rK}}\right]\otimes[1,j]\right)\mathbf{G}_l$, respectively, where $\check{\mathbf{b}}_p$ is the pth column of $\mathbf{A}\boldsymbol{\Sigma}_l$, $\mathbf{A}=\mathbf{A}_t\odot\mathbf{A}_t$, $\mathbf{C}=\mathbf{C}_t\otimes\mathbf{C}_r$, $c_{tk}=a_{tk}+jb_{tk}$, $c_{rk}=a_{rk}+jb_{rk}$ and $\mathbf{G}_l=\mathrm{blkdiag}\{\underbrace{\mathbf{Ac}_l,\ldots,\mathbf{Ac}_l}_{4K}\}$.

5. Simulation results

In this section, some numerical simulations are presented to verify the effectiveness and advantages of the proposed method algorithm. The MUSIC-Like algorithm [11], ESPRIT-Like algorithm [12] and the CRB are used to compare with the proposed method. In the following cases, a narrowband bistatic MIMO radar with $M=8$ transmit antennas and $N=10$ receive antennas is used. At the transmit side, the mth transmitted waveform is the mth row of $\overline{\mathbf{S}}\in\mathbb{C}^{J\times J}$, where $\overline{\mathbf{S}}=(1+j)/\sqrt{2}\mathbf{H}_J$, and $\mathbf{H}_J$ is the $J\times J$ Hadamard matrix with $J=256$. Unless stated otherwise, it is assumed that the number of uncorrelated targets is known as $P=3$, three widely spaced targets are located at $(\varphi_1,\theta_1)=(-15^\circ,25^\circ)$, $(\varphi_2,\theta_2)=(0^\circ,5^\circ)$ and $(\varphi_3,\theta_3)=(20^\circ,-20^\circ)$. The root mean square error (RMSE) is used for angle estimation performance evaluation, which is calculated by the formula

$$\mathrm{RMSE}=\sqrt{\frac{1}{2QP}\sum_{p=1}^{P}\sum_{i=1}^{Q}\left[\left(\hat{\varphi}_{p,i}-\varphi_p\right)^2+\left(\hat{\theta}_{p,i}-\theta_p\right)^2\right]} \tag{27}$$

where $\hat{\varphi}_{p,i}$ and $\hat{\theta}_{p,i}$ are the estimation of DOD φ_p and DOA θ_p for the ith Monte Carlo trial, respectively. Q is the number of the Monte Carlo trials. The signal-to-noise ratio (SNR) is defined as $\mathrm{SNR}=10\log_{10}(\sum_{l=1}^{L}\|[\mathbf{C}_r\mathbf{A}_r]\boldsymbol{\Sigma}_l[\mathbf{C}_t\mathbf{A}_t]^{\mathrm{T}}\mathbf{S}\|_F^2/\sum_{l=1}^{L}\|\mathbf{W}(t_l)\|_F^2)$. The spatial grid of the MUSIC-based methods is 0.001° and $Q=200$ is used in the following simulations.

In the first simulation, we first investigate the RMSE of angle estimation for $P=3$ widely spaced targets with the following two cases: (1) $K=1$ with $[c_{t0},c_{t1}]=[1,0.2+j0.0061]$ and $[c_{r0},c_{r1}]=[1,0.15+j0.0251]$. (2) $K=2$ with $[c_{t0},c_{t1},c_{t2}]=[1,0.7+j0.002,0.2+j0.061]$ and $[c_{r0},c_{r1},c_{r2}]=[1,0.6+0.j0121,0.15+j0.0251]$. The number of pulses is $L=50$. Fig. 1 shows the RMSE of different methods versus SNR for the case (1), and the RMSE of different methods versus SNR in case (2) is shown in Fig. 2. As shown in Figs. 1 and 2, compared with both of ESPRIT-Like and MUSIC-Like algorithms, the angle estimation of the proposed method is superior and closer to CRB. The reason is that the multidimensional structure of the received data and forward–backward averaging technique are taken into account, which allow us to suppress the noise more efficiently than SVD/EVD technique. Furthermore, it can be seen that the MUSIC-Like algorithm provides better angle estimation performance than ESPRIT-Like algorithm at high SNR region for the case (1). But it fails to work in case (2) owing to angle ambiguity, and the reason is shown in [12].

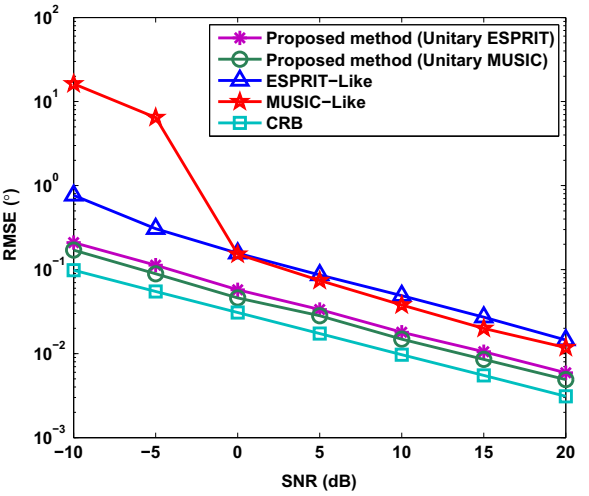

Fig. 1. RMSE of angle estimation versus SNR ($P=3$ widely spaced targets, $K=1$).

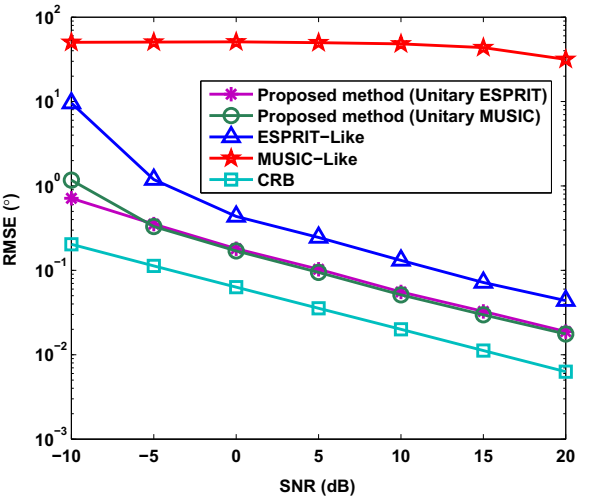

Fig. 2. RMSE of angle estimation versus SNR ($P=3$ widely spaced targets, $K=2$).

The second simulation is carried out to evaluate the angle estimation performance for $P=2$ closely spaced targets, where two targets are located at $(\varphi_1,\theta_1)=(5^\circ,0^\circ)$ and $(\varphi_2,\theta_2)=(10^\circ,-5^\circ)$. The number of pulses is $L=50$ and the mutual coupling is set as in case (1). Fig. 3 shows that the RMSE of different methods versus SNR for two closely targets. As seen in Fig. 3, compared with ESPRIT-Like and MUSIC-Like algorithms, the proposed methods (based on unitary MUSIC and unitary ESPRIT) provide better angle estimation performance, especially at low SNR region,

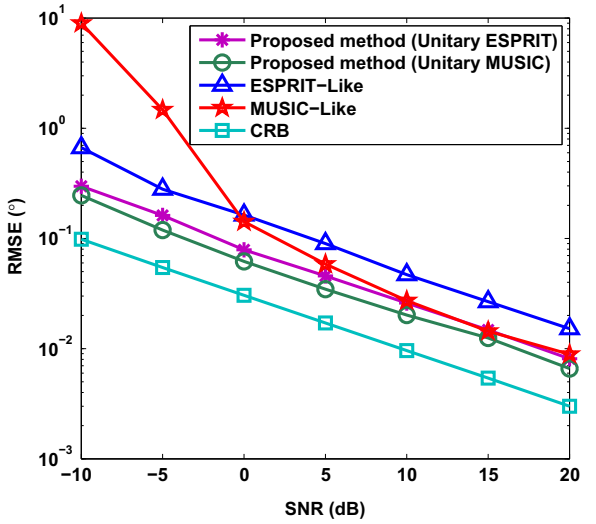

Fig. 3. RMSE of angle estimation versus SNR ($P=2$ closely spaced targets, $K=1$).

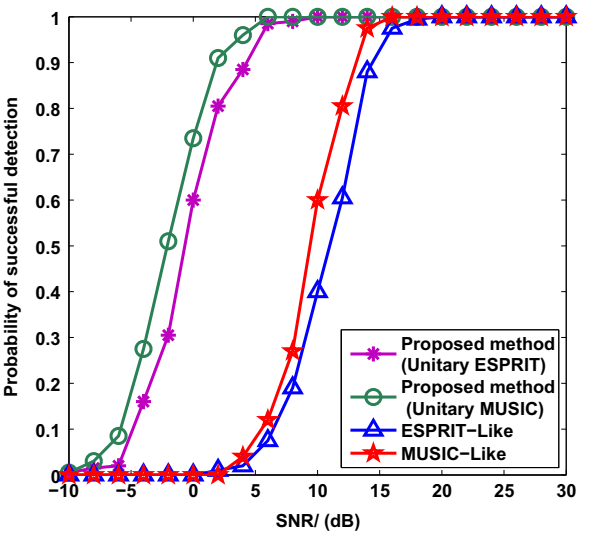

Fig. 5. Probability of successful detection versus SNR ($P=3$ widely spaced targets, $K=1$).

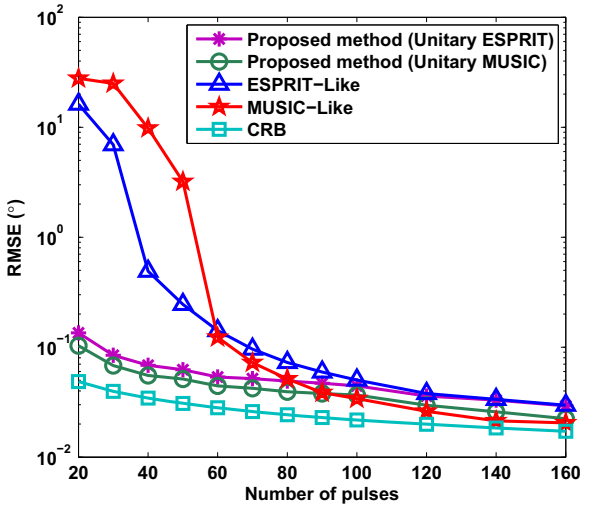

Fig. 4. RMSE of angle estimation versus pulses ($P=3$ widely spaced targets, $K=1$).

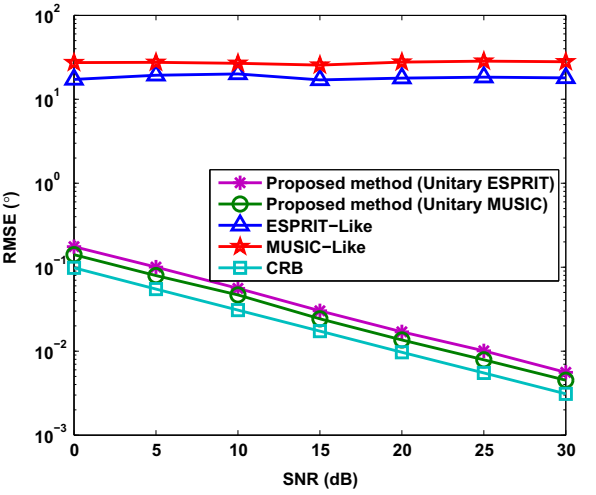

Fig. 6. The RMSE of different methods with two coherent targets ($P=3$ widely spaced targets, $K=1$).

which indicates that the proposed methods have higher resolution than both of ESPRIT-Like and MUSIC-Like algorithms.

The third simulation is carried out to evaluate the RMSE of different methods versus pulses for $P=3$ widely spaced targets, where SNR is 5 dB and the mutual coupling is set as in case (1). It can be seen from Fig. 4 that the angle estimation performance of the proposed methods (based on unitary MUSIC and unitary ESPRIT) is better than both ESPRIT-Like and MUSIC-Like algorithms with lower pulses. In larger pulse number case, the proposed method (based on unitary ESPRIT) provides almost same performance with ESPRIT-Like algorithm, and the MUSIC-Like algorithm has slightly better angle estimation performance than the proposed method based on unitary MUSIC-Like algorithm. However, the MUSIC-Like algorithm is only effective for small number of the nonzero mutual coupling coefficients, which has been shown at the first simulation.

The fourth simulation considers the probability of successful detection of different methods for $P=3$ widely spaced targets, where the number of pulses is $L=50$ and the mutual coupling is set as in case (1). All targets can be seen as successful detection when the absolute of DOD and DOA for all targets is within 0.1°. As seen in Fig. 5, all the methods show the 100% successful detection at high SNR region. The probability of successful detection for each method begins to drop at a certain point, which is defined as SNR threshold. It also can be seen that the proposed methods (based on unitary MUSIC and unitary ESPRIT) provide lower SNR threshold than MUSIC-Like and ESPRIT-Like algorithms. This is a direct result of the improved accuracy in the proposed method.

The fifth simulation considers the angle estimation performance of different methods for three widely spaced coherent targets with $L=50$, where the first two targets are coherent but uncorrelated with the third target, and the mutual coupling is set as in case (1). As seen in Fig. 6, it is indicated thatboth of MUSIC-Like and ESPRIT-like algorithms fail to work with two coherent targets case. However, the proposed methods (based on unitary MUSIC and unitary ESPRIT) are effective and provide accurate angle estimation performance, and the angle estimation performance of them is close to CRB.

6. Conclusion

In this paper, we proposed a tensor-based real-valued subspace approach for angle estimation in bistatic MIMO radar with unknown mutual coupling. The sub-tensor without the effect of mutual coupling can be extracted from the tensor data by utilizing the special structure of mutual coupling matrix with uniform linear array, then a signal subspace obtained from the real-valued tensor is formulated to estimate the DOD and DOA. Due to exploit of the multidimensional structural information of the received data and forward–backward averaging technique, the proposed method provides better angle estimation performance than MUSIC-Like and ESPRIT-Like algorithms at small pulses case and lower SNR case, and can be suitable for coherent targets. Numerical examples are presented to confirm the advantages of the proposed method.

Acknowledgements

This work is supported by the New Century Excellent Talents Support Program (NCET-11-0827), China Postdoctoral Science Foundation Grant (2014M550182), Fundamental Research runs for the Central Universities (HEUCFX-41308), Heilongjiang Postdoctoral Special Fund (LBH-TZ0410)and Innovation of Science and Technology Talents in Harbin (2013RFXX-J016).

References

[1] H. Krim, M. Viberg, Two decades of array signal processing research: the parametric approach, IEEE Signal Process. Mag. 13 (4) (1996) 67–94.
[2] R. Roy, T. Kailath, ESPRIT—estimation of signal parameters via rotational invariance techniques, IEEE Trans. Acoust., Speech Signal Process. 37 (3) (1989) 955–984.
[3] R.O. Schmidt, Multiple emitter location and signal parameter estimation, IEEE Trans. Antennas Propag. 34 (3) (1986) 276–280.
[4] A.M. Haimovich, R. Blum, L. Cimini, MIMO radar with widely separated antennas, IEEE Signal Process. Mag. 25 (1) (2008) 116–129.
[5] J. Li, P. Stoica, MIMO radar with colocated antennas, IEEE Signal Process. Mag. 24 (5) (2007) 106–114.
[6] H. Yan, J. Li, G. Liao, Multitarget identification and localization using bistatic MIMO radar systems, EURASIP J. Adv. Signal Process. (2008), 8, http://dx.doi.org/10.1155/2008/283483 (Article ID 283483).
[7] C. duofang, C. Baixiao, Q. Guodong, Angle estimation using ESPRIT in MIMO radar, Electron. Lett. 44 (12) (2008) 770–771.
[8] J. Chen, H. Gu, W. Su, Angle estimation using ESPRIT without pairing in MIMO radar, Electron. Lett. 44 (24) (2008) 1422–1423.
[9] W. Wang, X. Wang, H.R. Song, Y.H. Ma, Conjugate ESPRIT for DOA estimation in monostatic MIMO radar, Signal Process. 93 (2013) 2070–2075.
[10] W. Wang, X. Wang, X. Li, Y. Ma, Conjugate unitary ESPRIT algorithm for bistatic MIMO radar, IEICE Trans. Electron. 96 (1) (2013) 124–126.
[11] X. Liu, G. Liao, Direction finding and mutual coupling estimation for bistatic MIMO radar, Signal Process. 92 (2) (2012) 522–527.
[12] Z. Zheng, J. Zhang, J. Zhang, Joint DOD and DOA estimation of bistatic MIMO radar in the presence of unknown mutual coupling, Signal Process. 92 (12) (2012) 3039–3048.
[13] D. Nion, N.D. Sidiropoulos, Tensor algebra and multidimensional harmonic retrieval in signal processing for MIMO radar, IEEE Trans. Signal Process. 58 (11) (2010) 5693–5705.
[14] Y. Cheng, R. Yu, H. Gu, W. Su, Multi-SVD based subspace estimation to improve angle estimation accuracy in bistatic MIMO radar, Signal Process. 93 (7) (2013) 2003–2009.
[15] L.D. Lathauwer, B.D. Moor, J. Vandewalle, A multilinear singular value decomposition, SIAM J. Matrix Anal. Appl. 21 (4) (2000) 1253–1278.
[16] T.G. Kolda, B.W. Bader, Tensor decompositions and applications, SIAM Rev. 51 (3) (2009) 455–500.
[17] M. Haardt, F. Roemer, G. Del Galdo, Higher-order SVD-based subspace estimation to improve the parameter estimation accuracy in multi-dimensional harmonic retrieval problems, IEEE Trans. Sginal Process. 56 (7) (2008) 3198–3213.
[18] M. Pesavento, A.B. Gershman, M. Haardt, Unitary root-MUSIC with a real-valued eigendecomposition: a theoretical and experimental performance study, IEEE Trans. Sginal Process. 48 (5) (2000) 1306–1314.
[19] M. Haardt, J.A. Nossek, Unitary ESPRIT: how to obtain increased estimation accuracy with a reduced computational burden, IEEE Trans. Sginal Process. 43 (5) (1995) 1232–1242.
[20] M.D. Zoltowski, M. Haardt, C.P. Mathews, Closed-form 2-D angle estimation with rectangular arrays in element space or beamspace via unitary ESPRIT, IEEE Trans. Sginal Process. 42 (2) (1996) 316–328.
[21] G.H. Golub, C.F. van Loan, Matrix Computations, Johns Hopkins University Press, Baltimore, 1996.